# High Resolution Topography Along 40 km of the Southern San Andreas Fault

Michael P. Bunds[1], Chelsea Scott[2], Vickie Jiu-Chi Lee[3], and Brigham Whitney[1]
[1]Department of Earth Science, Utah Valley University [2]School of Earth and Space Exploration, Arizona State University [3]Department of Geosciences, Virginia Polytechnic Institute

*GSA Digital Upload Draft*
*For a final version of this poster please visit*
*https://www.researchgate.net/profile/Michael-Bunds-2*

*GSA Digital Upload Draft*
*For a final version of this poster please visit*
*https://www.researchgate.net/profile/Michael-Bunds-2*

## Project Overview

**Get the Data:** https://doi.org/10.5069/G94M92RG, https://opentopography.org/news/new-sfm-data-over-southern-san-andreas-fault-ca

### Overview

- **We acquired a new high resolution topography (HRT) dataset along 40 km of the Southern San Andreas from north of Painted Canyon to Bombay Beach that is available on OpenTopography**
- Generated with sUAS RGB photographs and structure-from-motion (SfM) processing, and georeferencing from onboard-sUAS dGNSS with 3.5 days field work and 3 days processing
- Point cloud (246 pts/m$^2$, 8.4 x 10$^9$ total points, ~30 km$^2$), orthomosaic (4 cm pixels), DEM (10 cm pixels). (Compare to B4 LiDAR: 5.7 x 10$^9$ points total, ~4 pts/m$^2$)
- Refined methodology to rapidly collect well-georeferenced HRT and orthoimagery of large area following a surface-rupturing earthquake

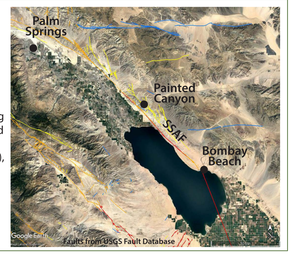


### Motivation

- Coachella section of Southern San Andreas fault (SSAF) is an active fault that poses significant seismic hazard in Southern California
- Make HRT dataset available to the community
- Pre-event dataset for future surface-rupturing earthquake
- HRT dataset useful to examine fault zone geology and geomorphology
- B4 airborne LiDAR was collected in 2005 with now old technology
- SSAF is accessible and low vegetation so amenable to sUAS-SfM
- Refine ability to rapidly acquire large HRT dataset quickly

### Field Data Collection

- 3. 5 days in the field
- 4 people, only 2 are necessary
- 1 vehicle
- GNSS reference station established each day (Septentrio PolaRXS receiver + Trimble Zephyr Geodetic II antenna). Locations marked by drilling holes in boulders, so may be possible to reoccupy in future
- 22 ~1-hour flights (sUAS managed with Sensefly eMotion software)
- 15773 aerial photographs collected
- sUAS: Sensefly eBee Plus fixed-wing, onboard multi-frequency dGNSS @ 1 Hz (PPK), SODA 20 MPixel camera, 8 batteries
- Photo target overlap: 70% longitudinal and 75% lateral
- Checkpoints: 24 with target (allows horizontal uncertainty check), 151 bare Earth


### SfM and dGNSS Processing

Preliminary processing was done each night in the field on 3 GPU-equipped laptops. Final processing was done at UVU following the methods below.

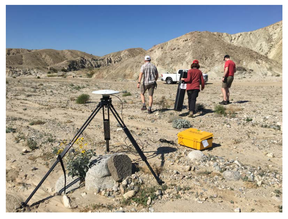

**dGNSS**

- Reference station locations determined using OPUS (National Geodetic Survey Online Positioning User Service), with precise ephemeri and 4.3 - 10 hour occupation times
- 1 Hz dGNSS positions of sUAS found using Sensefly eMotion software (Septentrio), PPK method, relative to our local reference stations
- eMotion (Septentrio) interpolates each camera position from 1 Hz dGNSS results, photograph time stamps, and orientation of sUAS (to calculate offset between camera and GNSS antenna)
- Positions determined in ITRF2014 horizontal reference frame and ellipsoidal heights

**Structure-from-Motion (SfM)**

- SfM processing done in Agisoft Metashape Pro
- Tie points / sparse cloud built on 'highest'
- Camera dGNSS positions added
- Camera models optimized and large uncertainty tie points removed iteratively with repeated optimizations
- Dense cloud built on 'high'
- Vertical bias relative to checkpoints was removed (~3 cm; typical of models georeferenced with camera positions)
- Adjustments were made to two problem areas for which onboard dGNSS failed
- Hardware: suite of five purpose-built workstations run as a parallel-processing cluster (52 hyper-threaded CPU cores, 12 NVIDIA GPUs [4 x 2080, 4 x 1080, 4 x 970]; approximately 48 hrs computing time for camera alignment + dense cloud generation.

**Quality Control**

- Checkpoints were measured with PPK dGNSS relative to our local reference stations. 155 total; 123 on bare earth, 28 with targets that allow horizontal root-mean-square-error calculation
- Vertical RMSe: 3.3 cm (relative to 155 checkpoints)
- Horizontal RMSe: 1.9 cm (relative to 28 checkpoints with targets)

Dataset Parameters Summary

| Parameter | SSAF topographic model |
|---|---|
| Total points | 8.43 x 10$^9$ |
| Coverage area | 34.3 km$^2$ |
| Average point density | 246 points/m$^2$ |
| Photograph count | 15773 |
| Average GSD | 0.034 m |
| Number of GCPs | 4 |
| Number of checkpoints | 155 |
| Horizontal Checkpoint RMS Error (From 28 checkpoints) | 0.019 m |
| Vertical Checkpoint RMS Error (From 155 checkpoints) | 0.033 m |
| DSM resolution | 0.1 m |
| Orthomosaic resolution | 0.040 m |
| Horizontal reference frame – point clouds, DSMs and orthomosaics | WGS UTM Zone 11 (EPSG 32611) from IGS14, epoch 2020.131 |
| Vertical reference frame | IGS14 Ellipsoid |
| Field data collection date | February, 2020 |

## Dataset Coverage


## Example Imagery

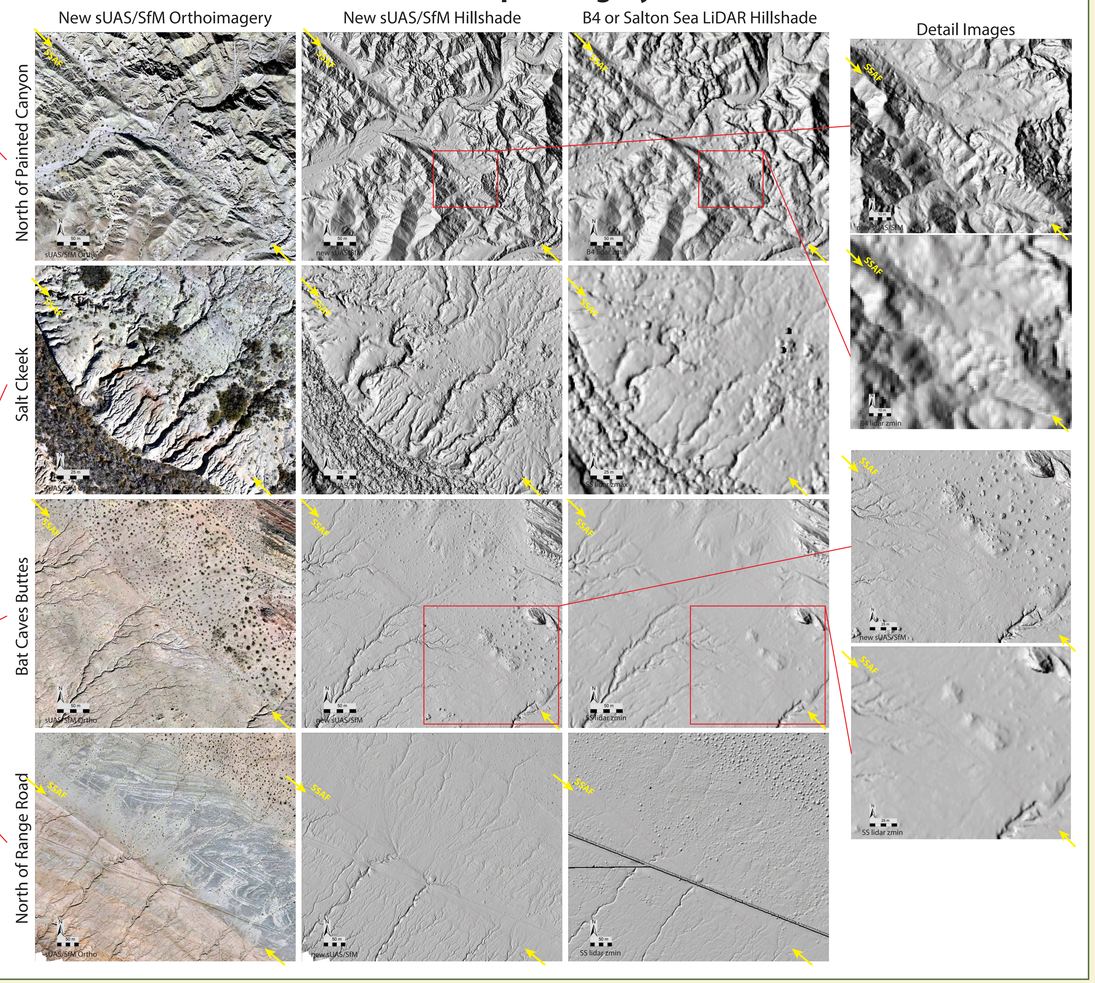


## Change Detection

Imaged areas outlined in yellow on strip map to left

3D differencing between our sUAS topography and the older lidar data sets that cover overlapping areas can be performed using new tools on OpenTopography that employ the iterative closest point method (ICP; Scott et al., 2021). Below, we show results from that method and raster math differencing between the 2005 B4 airborne lidar with our 2020 sUAS digital surface model. The results show cultural changes near Mortmar, and fluvial activity and construction near Painted Canyon and along the Coachella Canal. We have not detected , although additional 3D differencing may show fault creep as has been done for the central San Andreas fault (Scott et al., 2020).

In the event of a surface rupturing earthquake, the B4 lidar and our dataset will be complementary pre-event datasets given their varying spatial resolution, aperture, texture, error sources, and RGB color information in our data. Additional sUAV surveys following the earthquake could also be incorporated into differencing studies.

**ICP 3D differencing** divides 'before' and 'after' point clouds into windows and calculates vertical and horizontal displacement and rotation of the imaged surface in each window by matching the two point clouds. It is a powerful tool for quantitative estimation of tectonic an other displacements of the ground surface.

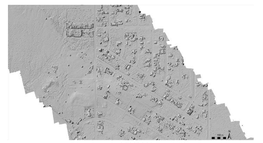

2020 sUAS

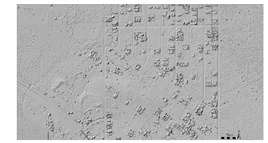

2005 B4 lidar

Surfside ICP Differencing Using OpenTopography Tools

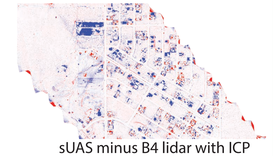

sUAS minus B4 lidar with ICP

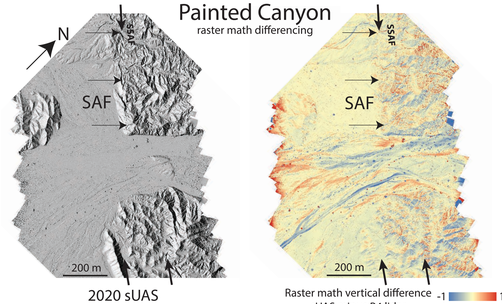


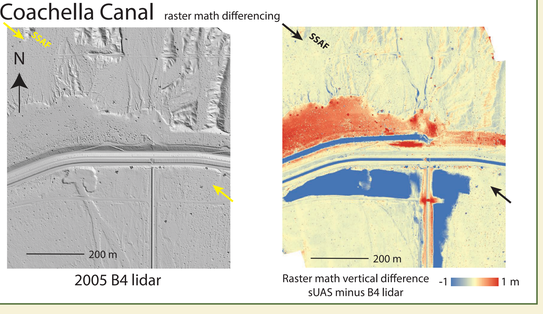


## Opportunities and Challenges

*Opportunities*

- Ability to cover > 10 km$^2$ per day in field; onboard dGNSS provides excellent georeferencing with much less labor than GCPs
- Rapid preliminary processing
- Rapid high resolution processing with cluster of high-performance machines
- **Potential to quickly produce large HRT data set(s) following a surface-rupturing event**

*Challenges*

- Poor or absent onboard dGNSS data for two flights
- Maintaining visual contact with sUAS, access to launch sites on fault
- Georeferencing offset between days
- Potential for sUAS damage
- Ability to upload ~5000 photos / day to remote server

**References**

Bevis, M. and Hudnut, K. (2005): B4 Lidar Project: Airborne Laser Swath Mapping (ALSM) survey of the San Andreas Fault (SAF) system of central and southern California, including the Banning segment of the SAF and the San Jacinto fault system. National Center for Airborne Laser Mapping (NCALM), U.S. Geological Survey, the Ohio State University, and the Southern California Integrated GPS Project. Distributed by OpenTopography. https://doi.org/10.5066/F7TQ5ZQ6. Accessed: 2020-09-07.

Salton Sea LiDAR Collection, 2010, U.S. Geological Survey. Distributed by OpenTopography. https://doi.org/10.5069/G9V985ZF. Accessed 2020-09-07.

Scott, C., Bunds, M.P., Shirzaei, M., Toke, N., 2020, Creep along the Central San Andreas Fault from Surface Fractures, Topographic Differencing, and InSAR Imagery, Journal of Geophysics, https://doi.org/10.1029/2020JB019762.

Scott, C., Phan, M., Nandigam, V., Crosby, C., Arrowsmith, J.R., 2021, Measuring change at Earth's surface: On-demand vertical and three- dimensional topographic differencing implemented in OpenTopography, GeoSphere, https://doi.org/10.1130/GES02259.1

U.S. Geological Survey and California Geological Survey, Quaternary fault and fold database for the United States, accessed 2020-09-01, at: https://www.usgs.gov/natural-hazards/earthquake-hazards/faults.

**Acknowledgements**
We are grateful for support from the NSF & SCEC (to Scott, SCEC award 19123), and the UVU Office of Engaged Learning & College of Science (awards to Bunds). We also thank NVIDIA for an educational GPU grant and Sensefly for educational equipment pricing. We thank OpenTopography for hosting the dataset.

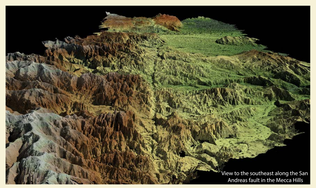


**Get the Data:**
https://doi.org/10.5069/G94M92RG
https://opentopography.org/news/new-sfm-data-over-southern-san-andreas-fault-ca